NASA/TM—2016-219118

Monte Carlo Simulation of a Knudsen Effusion Mass Spectrometer Sampling System

Michael J. Radke
Case Western Reserve University, Cleveland, Ohio

Nathan S. Jacobson
Glenn Research Center, Cleveland, Ohio

October 2016

NASA STI Program . . . in Profile

Since its founding, NASA has been dedicated to the advancement of aeronautics and space science. The NASA Scientific and Technical Information (STI) Program plays a key part in helping NASA maintain this important role.

The NASA STI Program operates under the auspices of the Agency Chief Information Officer. It collects, organizes, provides for archiving, and disseminates NASA's STI. The NASA STI Program provides access to the NASA Technical Report Server—Registered (NTRS Reg) and NASA Technical Report Server—Public (NTRS) thus providing one of the largest collections of aeronautical and space science STI in the world. Results are published in both non-NASA channels and by NASA in the NASA STI Report Series, which includes the following report types:

- TECHNICAL PUBLICATION. Reports of completed research or a major significant phase of research that present the results of NASA programs and include extensive data or theoretical analysis. Includes compilations of significant scientific and technical data and information deemed to be of continuing reference value. NASA counter-part of peer-reviewed formal professional papers, but has less stringent limitations on manuscript length and extent of graphic presentations.

- TECHNICAL MEMORANDUM. Scientific and technical findings that are preliminary or of specialized interest, e.g., "quick-release" reports, working papers, and bibliographies that contain minimal annotation. Does not contain extensive analysis.

- CONTRACTOR REPORT. Scientific and technical findings by NASA-sponsored contractors and grantees.

- CONFERENCE PUBLICATION. Collected papers from scientific and technical conferences, symposia, seminars, or other meetings sponsored or co-sponsored by NASA.

- SPECIAL PUBLICATION. Scientific, technical, or historical information from NASA programs, projects, and missions, often concerned with subjects having substantial public interest.

- TECHNICAL TRANSLATION. English-language translations of foreign scientific and technical material pertinent to NASA's mission.

For more information about the NASA STI program, see the following:

- Access the NASA STI program home page at http://www.sti.nasa.gov

- E-mail your question to help@sti.nasa.gov

- Fax your question to the NASA STI Information Desk at 757-864-6500

- Telephone the NASA STI Information Desk at 757-864-9658

- Write to:
  NASA STI Program
  Mail Stop 148
  NASA Langley Research Center
  Hampton, VA 23681-2199

NASA/TM—2016-219118

Monte Carlo Simulation of a Knudsen Effusion Mass Spectrometer Sampling System

Michael J. Radke
Case Western Reserve University, Cleveland, Ohio

Nathan S. Jacobson
Glenn Research Center, Cleveland, Ohio

National Aeronautics and
Space Administration

Glenn Research Center
Cleveland, Ohio 44135

October 2016

Acknowledgments

We are grateful to Evan Copland, formerly of NASA Glenn, now with CSIRO in Melbourne, Australia, for adapting the magnetic sector mass spectrometer at NASA Glenn to restricted collimation. We are also grateful to Edward A. Sechkar, ZIN Technologies/ NASA Glenn Group and Benjamin Kowalski, NASA Glenn, for assistance with the VBA code. Helpful discussions with Christian Chatillon, CNRS, SIMAP, Grenoble, France, are also appreciated. This work was sponsored by the Transformative Tools and Technologies Project under the Transformative Aeronautics Concepts Program.

Level of Review: This material has been technically reviewed by technical management.

Available from

NASA STI Program
Mail Stop 148
NASA Langley Research Center
Hampton, VA 23681-2199

National Technical Information Service
5285 Port Royal Road
Springfield, VA 22161
703-605-6000

This report is available in electronic form at http://www.sti.nasa.gov/ and http://ntrs.nasa.gov/

Monte Carlo Simulation of a Knudsen Effusion Mass Spectrometer Sampling System

Michael J. Radke
Case Western Reserve University
Cleveland, Ohio 44106

Nathan S. Jacobson
National Aeronautics and Space Administration
Glenn Research Center
Cleveland, Ohio 44135

Summary

Knudsen flow is easily simulated with a Monte Carlo method. In this study a Visual Basic for Excel (VBA) code is developed to simulate the molecular beam from a vaporizing solid. The system at NASA Glenn Research Center uses the "restricted collimation" method of Chatillon and colleagues, which consists of two apertures between the effusion cell and the ionizer. The diameter of the first aperture is smaller than the diameter of the effusion cell orifice, so the ionizer effectively "sees" only inside the effusion cell. The code is able to calculate the transmission coefficient through the cell orifice, through the cell orifice and the first aperture, and through the cell orifice and first and second apertures. Calculated transmission coefficients through the cell orifice are compared with tabulated values to validate the code. Then transmission coefficients are calculated through the cell orifice and both apertures to the ionizer. This allows the geometry (aperture spacing and diameters) of the sampling system to be optimized. Calculated transmission factors are also compared to literature values calculated via an analytic method.

1.0 Introduction

Knudsen effusion mass spectrometry (KEMS) is a well-established technique for sampling high-temperature vapors from a Knudsen cell (Refs. 1 to 3). A typical Knudsen cell is illustrated in Figure 1. The sample cell is heated uniformly, and an equilibrium vapor develops above the condensed phase. The effusion orifice has a well-defined geometry and directs a molecular beam composed of this vapor into the ionizer of a mass spectrometer. The requirements for Knudsen sampling include a cell orifice with a Knudsen number (ratio of the mean free path to orifice diameter) of 10 or greater. Thus molecule wall collisions dominate over molecule-molecule collisions, and the vapor in the molecular beam is representative of the vapor above the condensed phase.

Recently, Chatillon and coworkers have discussed a novel method of sampling from a Knudsen cell (Refs. 4 to 6). Their method is termed "restricted collimation" and involves two collimating apertures above the cell effusion orifice. The first is in the plate that separates the Knudsen cell chamber from the ionizer. Chatillon terms this the "field aperture." The field aperture is necessarily smaller than the Knudsen cell orifice, so that the ionizer effectively "sees" only the inside of the Knudsen cell. The second is right below the ionizing filament and is termed the "source aperture." The advantages of this restricted collimation configuration is that background is minimized. This is illustrated in Figure 2. Such sampling is particularly useful in multi-cell instruments, to limit cross-over of molecular beams from adjacent cells.

Chatillon and coworkers have modeled restricted collimation (Refs. 4 to 6) with equations analogous to the decay of light intensity. Molecular beams are analogous to transmission of light, a stream of photons. Many of the equations developed for light are readily applicable to these molecular beams. First, note that the flux decays as $1/a^2$, where a is the distance from the source to the receiver. The basic equations for flux received from a radiating element are derived in the paper and textbook by Walsh (Refs. 7 and 8). The problem germane to the collimation of a molecular beam in mass spectrometer is in

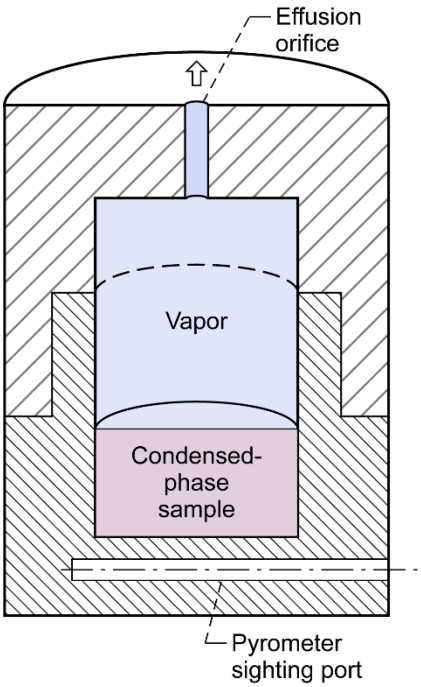

Figure 1.—Knudsen cell.

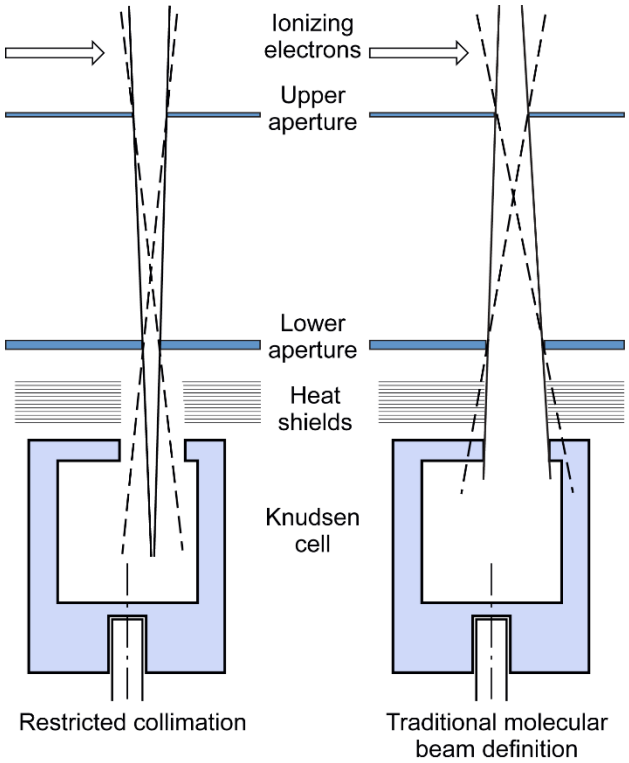

Figure 2.—Comparison of Knudsen cell restricted collimation to traditional molecular beam definition (adapted from Ref. 2). Note that the traditional method may also sample species evaporating from the cell lid and heat shields.

the transmission of the beam from one disc source to another co-axial disc source. The fraction of molecules F that leave the radiating disc and arrive at the receiving disk is given by

$$F(r_1, r_2, c) = \frac{(r_1^2 + r_2^2 + c^2) - \sqrt{(r_1^2 + r_2^2 + c^2) - 4r_1^2 r_2^2}}{2r_1^2} \tag{1}$$

Here c is the distance between the two disks, r_1 is the radius of the radiating disk, and r_2 is radius of the receiving disk. The quantity F is the unit of solid angle that reaches the second aperture (Ref. 7).

The two KEMS instruments at the NASA Glenn Research Center have been adapted for restricted collimation. The configuration from the cell to the ionizer is illustrated in Figures 3(a) and (b), for the magnetic sector instrument (Ref. 2) and quadrupole instrument, respectively. For both instruments, the Knudsen cell furnace chamber and ionizer chamber is separated by a copper plate. The field aperture in this plate is adjustable with a secondary piece, as shown in Figure 4. This is aligned with the source aperture using a laser.

Knudsen flow through pipes has been described analytically by many investigators (Refs. 9 and 10). Such descriptions of Knudsen flow are based on the analogous behavior of molecular flow to light and the cosine distribution law for vaporizing species. In 1960, Davis published a Monte Carlo simulation of Knudsen flow in pipes (Ref. 11). Since then, many investigators have further extended this Monte Carlo approach (Refs. 11 to 17). Today, because of the wide availability of high-speed desktop computers with multicore processors, Monte Carlo simulation is one of the easiest and most flexible ways to describe Knudsen flow.

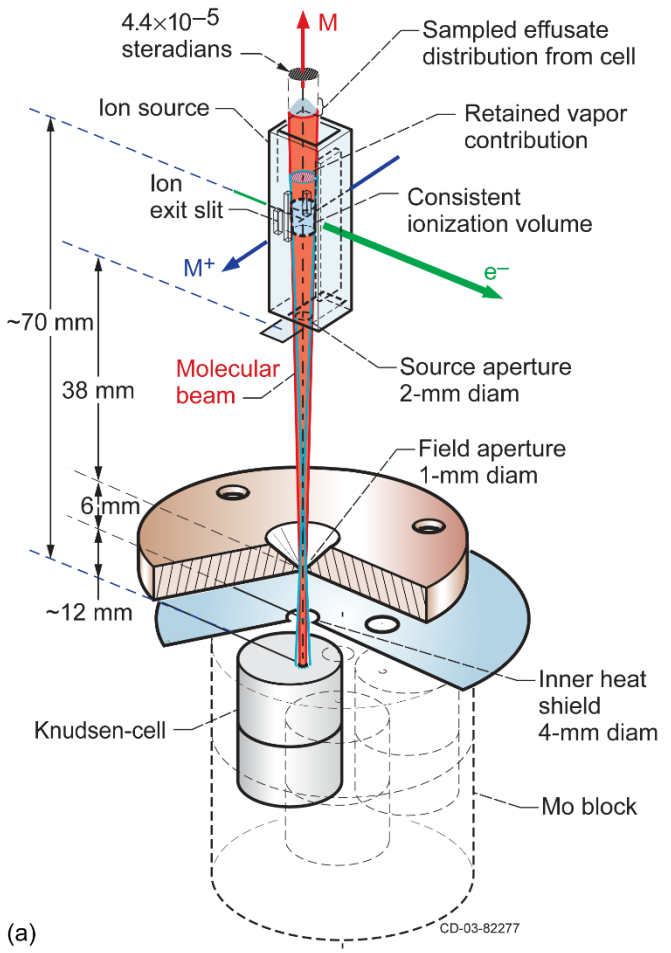

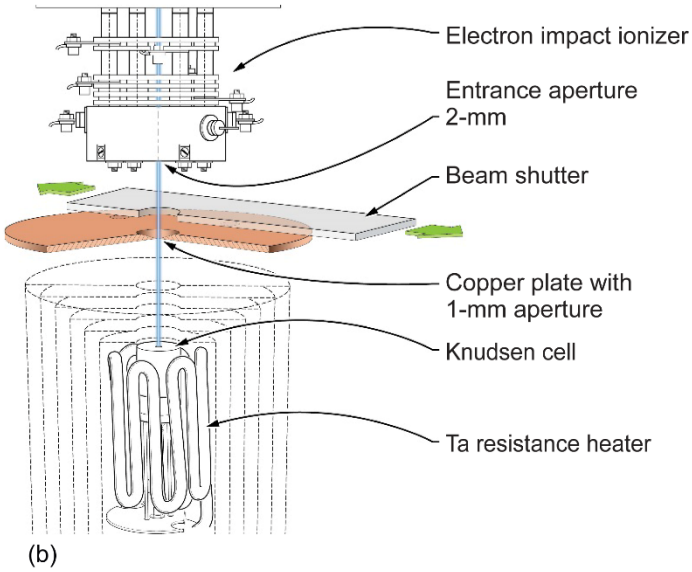

Figure 3.—Restricted collimation sampling for Glenn Knudsen effusion mass spectrometers. (a) Magnetic sector instrument (adapted from Ref. 2). (b) Quadrupole instrument.

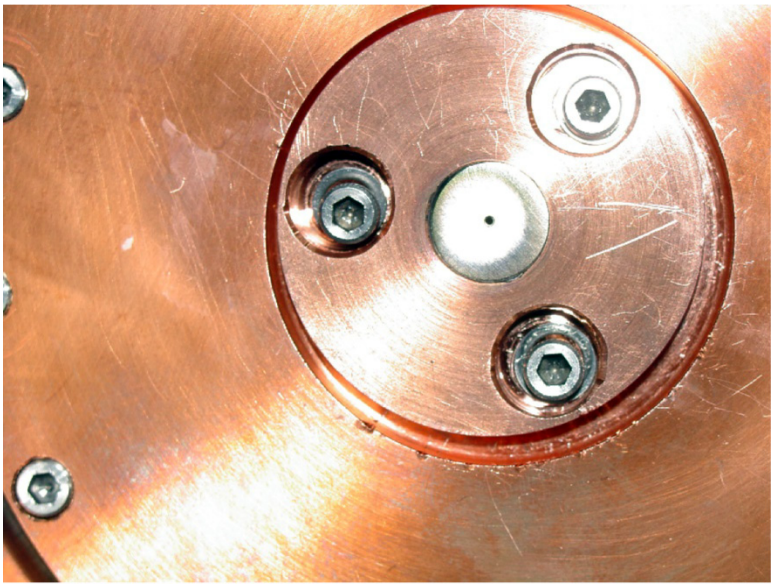

Figure 4.—Copper plate that separates Knudsen cell furnace chamber and ionization chamber in both Knudsen effusion mass spectrometry instruments at NASA Glenn. Flange in center contains field aperture and is adjustable in plane of flange.

In this report a Monte Carlo Knudsen flow simulation for pipes is adapted to model the vaporization of the condensed phase in the cell through the cell orifice and the two apertures. The code was adapted from an earlier FORTRAN code (Ref. 17) to Microsoft Visual Basic for Excel (VBA). Thus the code is readily run on any personal computer. It is very flexible, so that the various aperture diameters and distances can be adjusted to maximize molecular beam transmission. Apertures can be added or removed to calculate basic transmission through a channel or transmission through several apertures. Additionally, the pipe cross section can be changed from cylindrical to rectangular.

Initially, major equations are derived. A description of the code follows, with a model of the systems at Glenn Research Center (Figs. 3(a) and (b)). Finally, the calculated transmission factors for various configurations are compared with tabulated values, determined from analytical expressions and experiments. Nomenclature used in this report is listed in Appendix A.

2.0 Derivation of Equations for Starting Point and Trajectories

In this section the major equations are derived from solid geometry relations. The approach of Davis and others are followed (Refs. 11 and 17).

2.1 Solid Angles

The first step to describe a trajectory of a vaporizing molecule is to define a solid angle. Consider the hemisphere shown in Figure 5 where the angle with the x-axis θ varies uniformly from 0 to $\pi/2$ radians and the angle in the y,z-plane φ varies from 0 to 2π radians. An infinitesimal element of the solid angle, $d\omega$, is given by

$$d\omega = \sin\theta \, d\varphi \, d\theta \tag{2}$$

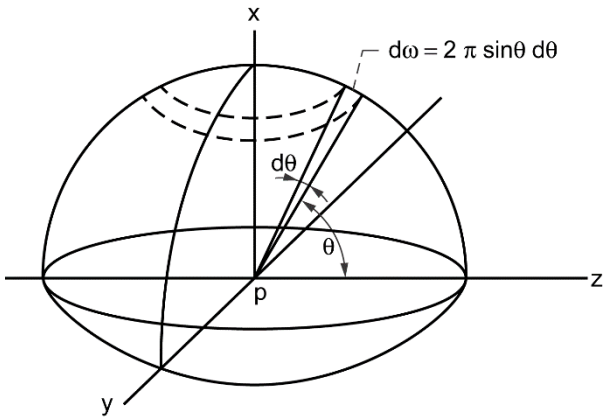

Figure 5.—Element of solid angle, dω. Starting point for trajectory of vaporizing molecule is "p."

We can define the solid angle as the surface area of a portion of a unit sphere. In our case only θ is specified and φ varies randomly from 0 to 2π radians, so this area becomes an infinitesimal band around the sphere, as shown in Figure 5. Thus the above expression simplifies to

$$\mathrm{d}\omega = 2\pi \sin\theta \, \mathrm{d}\theta \tag{3}$$

Suppose we want the amount of solid angle from 0 to θ. This is found by the integration:

$$\int \mathrm{d}\omega = \int_0^{\theta'} 2\pi \sin\theta \, \mathrm{d}\theta = 2\pi\left(1 - \cos\theta\right) \tag{4}$$

2.2 Cosine Distributions

Although φ is a uniformly distributed random variable between 0 and 2π radians, θ must follow a known cosine distribution. In other words, the elemental flux of molecules, $\mathrm{d}N_\theta$ leaving a plane into a solid angle element dω with angle θ to the surface normal is proportional to the cosine of that angle:

$$\mathrm{d}N_\theta \propto \cos\theta \, \mathrm{d}\omega \tag{5}$$

Putting Equation (3) into Equation (5) above gives

$$\mathrm{d}N_\theta \propto 2\pi \cos\theta \sin\theta \, \mathrm{d}\theta \tag{6}$$

So the question is how to generate this distribution in a computer code. Following Davis (Ref. 11), we generate two uniformly distributed random numbers *R* between 0 and 1 and then select the larger of the two. This means that the larger the value of *R* is, the higher the probability of selecting it. If *P*(*R*) is the probability of selecting *R*, then

$$P(R) \, \mathrm{d}R = 2R \, \mathrm{d}R \tag{7}$$

Let $R = \cos\theta$, so now we have

$$P(\cos\theta)\,\mathrm{d}(\cos\theta) = 2\cos\theta \frac{\mathrm{d}(\cos\theta)}{\mathrm{d}\theta}\mathrm{d}\theta = 2\cos\theta \sin\theta \, \mathrm{d}\theta \tag{8}$$

This is the distribution required given in Equation (5). This distribution is used to determine the initial trajectory of the simulated molecules as well as their new trajectories after wall collisions.

2.3 Direction Cosines

In order to define the trajectory of a molecule, we need to assign it direction cosines. These are simply the cosines of the angles α, β, and γ that a vector makes with the x-, y-, and z-axes, respectively. The direction cosines can be expressed in terms of the spherical coordinates θ and φ, discussed previously:

$$\begin{aligned} \mu_1 &= \cos\alpha = \cos\varphi \ \sin\theta \\ \mu_2 &= \cos\beta = \sin\varphi \ \sin\theta \\ \mu_3 &= \cos\gamma = \cos\theta \end{aligned} \tag{9}$$

The cosine of θ is derived via the procedure discussed in Section 3.2. As noted, φ varies randomly from 0 to 2π. Von Neumann (Ref. 18) describes a method to derive trigonometric functions for angles varying uniformly between 0 and 2π without using the more computer-time-consuming functions (e.g., trigonometric functions and square roots). Consider a rectangle formed by random numbers *f* and *g*, which both vary uniformly between 0 and 1:

$$\sin\delta = \frac{\pm f}{\sqrt{f^2 + g^2}} \qquad \cos\delta = \frac{\pm g}{\sqrt{f^2 + g^2}} \tag{10}$$

The square roots in the denominators can be eliminated by using half-angle formulae:

$$\begin{aligned} \cos\varphi &= \cos 2\delta = 1 - 2\sin^2\delta \\ \sin\varphi &= 2\sin\delta\cos\delta \end{aligned} \tag{11}$$

In order to have φ vary from 0 to 2π, δ must vary from 0 to π. Thus define δ in a rectangle with sides

$$\begin{aligned} f &= 2R_1 - 1 \qquad 0 < R_1 < 1 \qquad -1 < f < 1 \\ g &= R_2 \qquad\quad 0 < g < 1 \end{aligned} \tag{12}$$

Finally, Equations (10) to (12) are combined to yield:

$$\begin{aligned} \cos\varphi &= \frac{(2R_1 - 1)^2 - R_2^2}{(2R_1 - 1)^2 + R_2^2} \\ \sin\varphi &= \frac{2(2R_1 - 1)R_2}{(2R_1 - 1)^2 + R_2^2} \end{aligned} \tag{13}$$

3.0 Method to Determine Trajectory Endpoints

The program traces the trajectory of each molecule. A distance criterion is used to determine if the molecule (1) strikes the wall, (2) escapes from the top, or (3) returns to the bottom. In the event of a wall collision, another trajectory is calculated. First the equations are derived for a cylinder and then extended to cover the additional collimating apertures in the system. An option for rectangular apertures is also discussed.

3.1 Simulation Geometry

The geometry of the simulation and its dimensions are selected by the user with the user interface shown in Figure 6. Each of the dimensions listed are variables to be entered in the code.

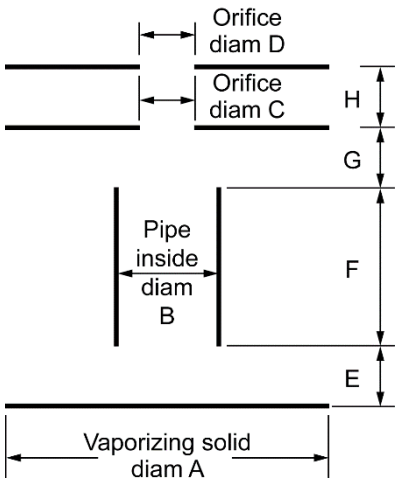

Figure 6.—Two-dimensional representation of simulated restricted collimation sampling system in Knudsen effusion mass spectrometer.

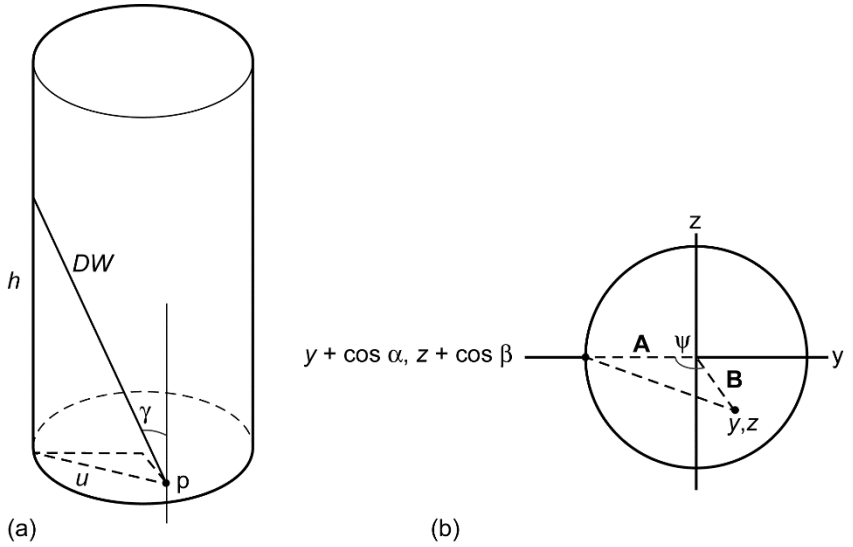

Figure 7.—Trajectory of molecule vaporizing from cylinder base. (a) Dimensions describing first flight of molecule. (b) Base of cylinder.

3.2 Initial Trajectory

Figure 7 illustrates a simple cylinder that has Cartesian coordinates defined as indicated: x is the center axis of the cylinder, and y and z are in a plane perpendicular to that center axis. This represents the orifice of the cell. The cosine distribution defining molecules initial trajectories must be oriented about the x-axis, and thus the first set of direction cosines is given as

$$\begin{aligned} \mu_1 &= \cos\gamma = \cos\theta \\ \mu_2 &= \cos\beta = \sin\varphi \, \sin\theta \\ \mu_3 &= \cos\alpha = \cos\varphi \, \sin\theta \end{aligned} \tag{14}$$

Here μ_1 is the direction cosine for the x-axis, μ_2 is the direction cosine for the y-axis, and μ_3 is the direction cosine for the z-axis.

Having defined the directions a molecule leaves a surface or a plane, now define the first trajectory. Consider the base of the cylinder. Define a completely random starting point. Place the origin at the center of the cylinder base, and set the radius of the cylinder equal to one. Then select a point

$$y_s = u = 2R_1 - 1 \qquad 0 < R_1 < 1 \qquad -1 < u < 1 \tag{15}$$

$$z_s = v = 2R_2 - 1 \qquad 0 < R_2 < 1 \qquad -1 < v < 1$$

subject to the condition that

$$y_s^2 + z_s^2 < 1 \tag{16}$$

where Equation (16) is the equation for a circle in the y,z-plane, representing an emissive surface at the bottom of the channel.

The first "flight" of a molecule is illustrated in Figure 7(a). The first question to be answered is whether the molecule strikes the wall or leaves the orifice. Following Davis (Ref. 11), this is done with a distance criterion. Two distances are calculated in the direction of the previously defined direction cosines—the distance from the base of the channel to the wall and the distance from the base to the top of the channel. Whichever distance is smaller determines the event that occurs: a wall collision or an escape from the channel. This method of distance comparison was determined to be much more efficient than computing and comparing angles of molecule trajectories, without sacrificing simulation accuracy. First consider the distance from the base of the cylinder to the wall, *DW*, as shown in Figure 7(a). Figure 7(b) illustrates projection to the base of the cylinder. From this figure,

$$\begin{aligned} (DW)^2 &= h^2 + u^2 \\ h^2 &= (DW)^2 \cos^2\gamma \end{aligned} \tag{17}$$

where *h* is the height of the collision point on the cylinder. The value of *u* (the length of the base in the right triangle formed with *DW* and *h*) can be expressed in terms of the angle Ψ between **A** and **B** (Fig. 7(b)) by the law of cosines:

$$\begin{aligned} u^2 &= A^2 + B^2 - 2AB\cos\Psi = 1 + y^2 + z^2 - 2\sqrt{y^2 + z^2}\cos\Psi \\ \cos\Psi &= \frac{\mathbf{A}\cdot\mathbf{B}}{AB} = \frac{y^2 + (DW)y\cos\beta + z^2 + (DW)z\cos\alpha}{\sqrt{y^2 + z^2}} \end{aligned} \tag{18}$$

Now determine *u* in terms of the direction cosines and *x* and *y*:

$$u^2 = 1 - (y^2 + z^2) - 2(DW)(y\cos\beta + z\cos\alpha) \tag{19}$$

Simplify this with the notation of Davis (Ref. 11):

$$\begin{aligned} D &= \left(y^2 + z^2\right) - 1 \\ Q &= y\cos\beta + z\cos\alpha \\ P &= \cos^2\alpha + \cos^2\beta \qquad 1 - P = \cos^2\gamma \end{aligned} \tag{20}$$

This gives a quadratic:

$$0 = P(DW)^2 + 2Q(DW) + D$$
$$DW = \frac{-Q}{P} \pm \sqrt{\frac{Q^2}{P^2} - \frac{D}{P}} \tag{21}$$

The distance to the wall of the cylinder, scaled to the y-direction cosine, is given by

$$SW = \frac{1}{\mu_2}\left(\frac{-Q}{P} \pm \sqrt{\frac{Q^2}{P^2} - \frac{D}{P}} \right) \tag{22}$$

The distance to the top of the cylinder, scaled to the x-direction cosine, is simple and given by

$$ST = \frac{L}{\cos\gamma} = \frac{L}{\mu_1} \tag{23}$$

where L is the length of the channel. As noted, the distance criterion is used to determine the event.

3.3 Trajectory After Wall Collision

The coordinates of the wall collision point are determined from the direction cosines:

$$\begin{aligned} x &= (DW)\cos\alpha \\ y &= y_{\text{old}} + (DW)\cos\beta \\ z &= z_{\text{old}} + (DW)\cos\gamma \end{aligned} \tag{24}$$

Once the molecule strikes the wall, it reflects diffusely off the surface with a cosine distribution about the normal to the tangent at that point (y_{new}, z_{new}). The molecule does not undergo specular reflection—and simply obey the law of reflection—because the surface of the channel is microscopically rough. A cosine distribution about the normal to the point of reflection is obtained by rotating the original coordinate system (which has the origin at the center of the base of the cylinder and the x-axis along the center of the cylinder).

The first step in doing so is to rotate the x-axis into the negative y-axis and the y-axis into the negative x-axis so

$$\begin{aligned} \mu_1 &= -\mu_2 \\ \mu_2 &= -\mu_1 \\ \mu_3 &= \mu_3 \end{aligned} \tag{25}$$

The next step is to rotate the y- and z-axes by an angle of transformation, ξ. The equations for rotation of the point (y_1,z_2) to the new coordinate system (y_1', z_2') are given by

$$\begin{aligned} y_1' &= y_1\cos\xi - z_1\sin\xi \\ z_1' &= y_1\cos\xi + z_1\sin\xi \\ x_1' &= x_1 \end{aligned} \tag{26}$$

Next cos ξ and sin ξ can be calculated as

$$\begin{aligned} \sin\xi &= \frac{y}{\sqrt{y^2 + z^2}} \\ \cos\xi &= \frac{z}{\sqrt{y^2 + z^2}} \end{aligned} \tag{27}$$

Note that the actual coordinates of the impact point are not being rotated. The only transformation that occurs is of the direction cosines, which define the new trajectory of the molecule after collision. The values of y_1 and z_1 are only used to calculate $\sin\xi$ and $\cos\xi$.

$$\begin{aligned} y_1 &= -\mu_1 \\ z_1 &= \mu_3 \\ \cos\beta &= -\mu_1(\sin\xi) - \mu_3(\cos\xi) = -\mu_1 y_{\text{new}} - \mu_3 z_{\text{new}} \\ \cos\gamma &= -\mu_1(\cos\xi) + \mu_3(\sin\xi) = -\mu_1 z_{\text{new}} + \mu_3 y_{\text{new}} \\ \cos\alpha &= -\mu_2 \end{aligned} \tag{28}$$

Also note that $\cos\alpha$ has been defined by Equation (24) above. Thus, Equation (28) defines a set of direction cosines such that the molecule desorbs after collision with a cosine distribution about the axis perpendicular to the tangent of the desorption point.

Now the issue is to determine the distance from the desorption point to (1) another wall collision, (2) the top of the channel, or (3) the bottom of the channel. Again the shortest distance is taken as the event. The distance to the wall is easily calculated from Equations (17) and (18). Now since the point is on the edge of the cylinder, $y^2 + z^2 = 1$, then $D = 0$ and the scale distance to the wall (Eq. (21)) simplifies to

$$(SW) = \frac{-2Q}{P} \tag{29}$$

The equation for the scaled distance to the top is

$$(ST) = \frac{L - x}{\mu_1} \tag{30}$$

The equation for the scaled distance to the bottom is

$$(SB) = \frac{x}{\mu_1} \tag{31}$$

If the calculated distance is negative, the molecule will never intersect with the object of interest, and the distance is assigned a very large number. As before, the shortest distance determines the event. If the molecule strikes a wall, a new collision is simulated like before. If the molecule passes out the bottom of the channel, the molecule is counted as returning to the start, and a new molecule's trajectory is simulated. Finally, if the molecule passes out the top of the channel, it is counted as an escape, and its trajectory can be traced through additional channels or apertures.

3.4 Trajectory Through Additional Aperture(s)

A molecule will pass through an aperture (with negligible thickness) if its radial distance from the central axis at the x-position of the aperture is less than the radius of the aperture. In other words,

$$y^2 + z^2 < r_{\text{ap}}^2 \tag{32}$$

Based on Figure 7(a), the equation for the scale distance to the first aperture from the last collision is

$$SA = \frac{\text{dist.}}{\mu_1} = \frac{(x - L) + G}{\mu_1} \tag{33}$$

where $(x - L)$ represents the remaining distance the molecule has to travel to escape the channel from its last collision and G, the distance between the top of the channel and the aperture. We can then calculate

the y and z positions of the molecule at the x-position of the aperture using the molecule's direction cosines and the previously calculated scale factor from Equation (32):

$$\begin{aligned} y &= \mu_2 \cdot SA \\ z &= \mu_3 \cdot SA \end{aligned} \tag{34}$$

Substituting Equations (34) into Equation (32) yields

$$(\mu_2 \cdot SA)^2 + (\mu_3 \cdot SA)^2 < r_{ap}^2 \tag{35}$$

If the inequality is satisfied, the molecule passes through the aperture. This process can be repeated for as many apertures as necessary, with the only change being the distance used to calculate the scale factor SA. For example, for the second aperture shown in Figure 6, the distance becomes $(x - L) + G + H$, where H is the distance between the two apertures.

3.5 Rectangular Channels and Apertures

The simulation procedure for rectangular channels and apertures is largely the same as for round ones, the major exception being the distance to wall collisions. First, calculate the distance from the starting point to y and z coordinates of the channel walls, illustrated in Figure 7:

$$\begin{aligned} SY &= \frac{(a/2) - y}{\mu_2} \\ SZ &= \frac{(b/2) - z}{\mu_3} \end{aligned} \tag{36}$$

As for cylindrical channels, the shorter of the two distances determines the wall collision. The coordinates of the collision are obtained by simply multiplying each of the direction cosines by the scale factor (SY or SZ) and adding these values to the previous coordinates.

Additionally, after a wall collision, the new cosine distribution simply needs to be rotated $\pi/2$ radians, such that the central axis of the distribution is normal to the surface on which the collision occurred. This is equivalent to setting y and z in Equation (27) to the appropriate values—either the half-width of the channel or zero. For a molecule striking the wall at $y = a/2$ this would mean $z = 0$, and

$$\begin{aligned} \cos\alpha &= -\mu_2 \\ \cos\beta &= -\mu_1 \\ \cos\gamma &= \mu_3 \end{aligned} \tag{37}$$

For apertures, the only difference is that a molecule successfully passes through when the position of a molecule in the y,z-plane is less than the half-width of the channel in either coordinate:

$$y < \left|\frac{a}{2}\right| \qquad z < \left|\frac{b}{2}\right| \tag{38}$$

rather than the check in Equation (31).

4.0 Results

First a series of calculations on simple cylindrical and rectangular channels is presented to compare to tabulated values and thereby verify proper operation of the code. Appendix B shows the input and output screens. Then the transmission factors for a typical restricted collimation mass spectrometer system are calculated and compared to the analytical approach used by Chatillon and coworkers (Refs. 4 and 6).

4.1 Calculated Transmission Factors

Transmission factors through cylindrical and rectangular channels have been calculated for a variety of geometries and show good agreement with tabulated transmission factors, as shown in Tables I and II (Refs. 19 and 20). Figure 8 shows the angular distribution of molecules effusing from cylindrical channels with various length-to-radius ratios (*l*/*r*). To create these plots, molecules are sorted into 1° bins according to the angle they make with the x-axis as they exit the channel. These counts are then normalized to the sine of the small increment of solid angle in Equation (2) and plotted on polar axes. The *l*/*r* of the channel has a strong effect on the distribution of exiting molecules, with large *l*/*r* creating a narrow beam of molecules, as opposed to the near ideal Cosine Law distribution of very low *l*/*r*.

TABLE I.—SELECTED TRANSMISSION FACTORS FOR CYLINDRICAL EFFUSION ORIFICES

Length-to-radius ratio, *L*/*r*	Simulation results, *W*	Tabulated values,[a] *W*	Difference, percent
0.2	0.90873	0.9092	−0.052
2	0.51322	0.5136	−0.074
4	0.35682	0.3589	−0.580
8	0.22542	0.2316	−2.668
20	0.10943	0.1135	−3.586
100	0.02549	0.0258	−1.202

[a]Source: Clausing (Ref. 19).

TABLE II.—TRANSMISSION FACTORS FOR KNUDSEN CELL RECTANGULAR EFFUSION ORIFICES

Column length per width, *l*/*b*	Transmission factor		Difference, percent
	Simulation result, *W*	Tabulated value,[a] *W*	
0.1	0.91314	0.9131	0.004
1	0.53643	0.5363	0.024
2	0.37831	0.3780	0.820
4	0.24236	0.2424	−0.017
10	0.12001	0.1195	0.427
40	0.03465	0.0346	0.145

[a]Source: Santeler and Boeckmann (Ref. 20).

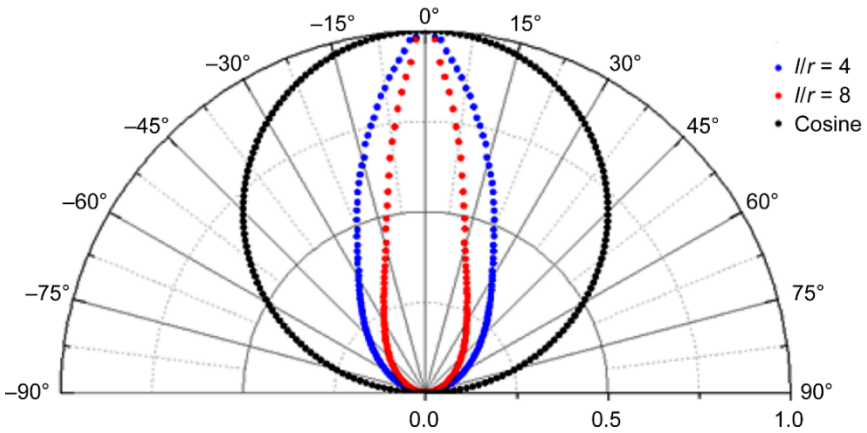

Figure 8.—Cosine distribution emerging from channel of different length-to-radius ratio *l*/*r*.

4.2 Calculated Properties for a Restricted Collimation Knudsen Effusion Mass Spectrometer

Table III contains the calculated properties of the KEMS geometry used at NASA Glenn shown in Figure 2 using 10^8 simulated molecules. A1 and A2 refer the lower and upper apertures, respectively. Only 11 percent of molecules effusing directly from the pipe do not undergo any wall collisions. However, the additional collimating apertures, A1 and A2, increase the proportion of molecules passing directly from the source to the mass spectrometer ionizer to 90 percent.

Figures 9(a) to (c) shows the views of the molecular path in a restricted collimation. In this simulation, 10^6 molecules were run. The vaporizing surface is at the bottom of the pipe. Figure 9(a) is a view of the first 50 molecular trajectories in the pipe. Figure 9(b) is a view of the whole beam and Figure 9(c) is a view from the top. The open circles are the molecules that made it through to the ionizer.

In Figure 10, the results of this method are compared to those from the analytical method used by Chatillon and coworkers (Ref. 6) to describe a restricted collimation system. The transmission factor, W, through the last aperture is plotted versus the source (upper) aperture diameter. As described by Chatillon and coworkers (Ref. 6), the diameter of the lower orifice necessarily changes for geometry considerations. The geometry they used was reproduced as close as possible for this calculation.

Vaporizing solid: 2.0-mm diameter at base of orifice
Cell orifice: 2.0-mm diameter; 2.0-mm thickness
Lower aperture: Diameter from Table 1 of Reference 6; 0.01-mm thickness; 10 mm from cell orifice
Upper aperture: Diameter from Table 1 of Reference 6; 0.01-mm thickness; 50 mm from cell orifice

TABLE III.—CALCULATED PROPERTIES FOR TYPICAL KNUDSEN EFFUSION MASS SPECTROMETRY CELL GEOMETRY AT NASA GLENN
[Length-to-radius ratio l/r = 5.33.]

Input values		
Pipe length, l_{pipe} = 4.0 mm	Diameter at lower aperture, d_{A1} = 1 mm	Distance between top of channel and lower aperture, G = 25.0 mm
Pipe diameter, d_{pipe} = 1.5 mm	Diameter at upper aperture, d_{A2} = 2 mm	Distance between lower and upper apertures, H = 37.7 mm

Simulation results			
Location	Transmission factor	Average number of collisions, $\bar{c}$	Percent without collisions, nc
Pipe	W_{pipe} = 0.2977	$\bar{c}_{pipe}$ = 7.36	nc_{pipe} = 11.2
Lower aperture	W_{A1} = 3.5×10^{-4}	$\bar{c}_{A1}$ = 7.9×10^{-4}	nc_{A1} = 86.4
Upper aperture	W_{A2} = 1.6×10^{-4}	$\bar{c}_{A2}$ = 3.4×10^{-4}	nc_{A2} = 90.1

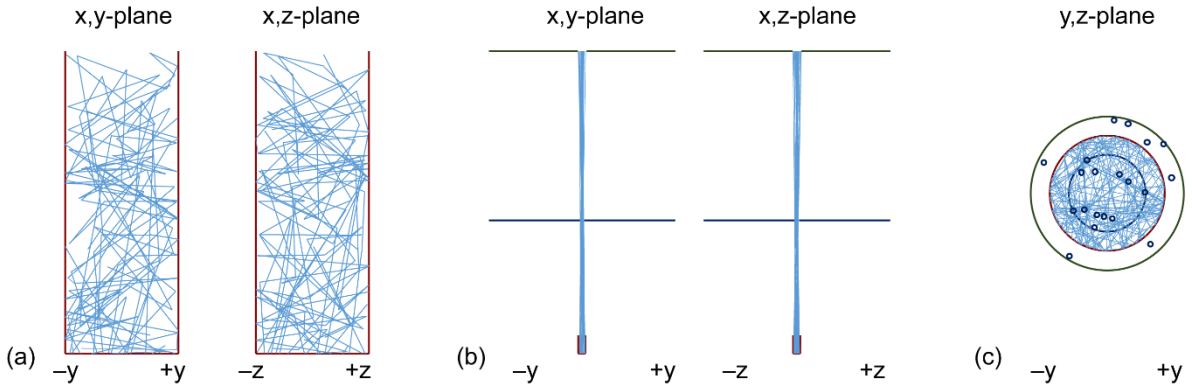

Figure 9.—Views of molecular trajectory from vaporizing surface to ionizer in Knudsen effusion mass spectrometer with restricted collimation. (a) Collisions within pipe. (b) Paths through apertures. (c) View from top. Circles are molecules that make it through upper orifice.

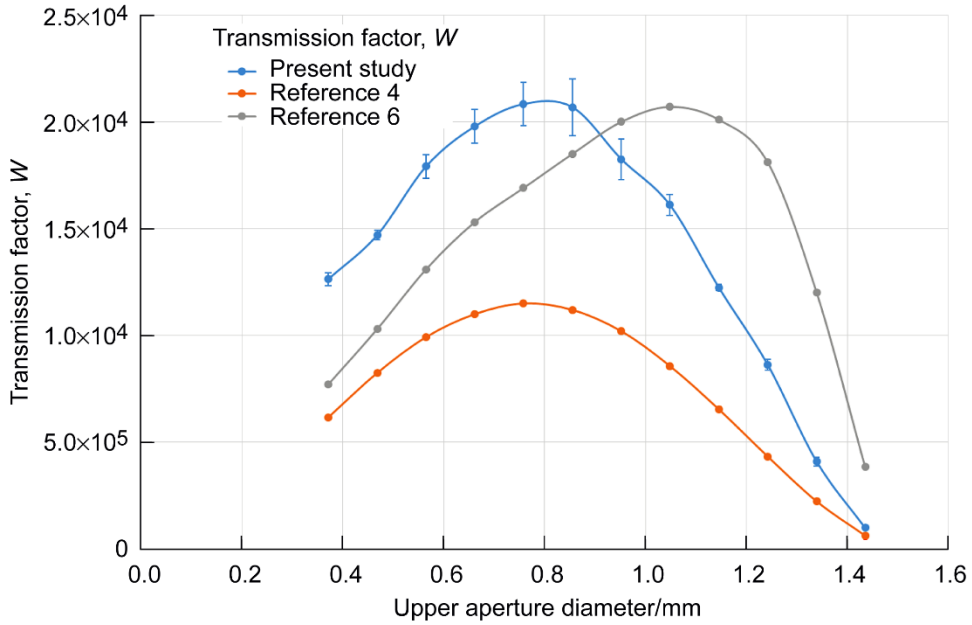

Figure 10.—Transmission factor of Knudsen effusion mass spectrometer with restricted collimation as function of upper aperture diameter.

The calculations herein show order-of-magnitude agreement with those of Chatillon and coworkers (Refs. 4 to 6). They also show maxima, as do those of Chatillon et al. The slightly different maxima with the two approaches needs to be explored further. The calculations of Chatillon and coworkers are based on the attenuation in beam strength described by Equation (1) and an integration over the solid angle shown in Figure 2(a). This approach treats the process more like "plug flow," and there are likely fundamental differences between this and the Monte Carlo approach where each trajectory is treated individually.

Further refinements to the Monte Carlo code are the ability to handle large sample sizes and the incorporation of molecule-molecule collisions. The code in VBA seems to be limited to ~1×10^8 trajectories. A more appropriate computer language would be necessary to increase the sample size. Molecule-molecule collisions can be incorporated by having the molecule randomly changing direction after traversing a mean free path. These changes can be incorporated into subsequent versions.

5.0 Conclusion

The existing Monte Carlo simulation allows for the fast (10^6 molecules in ~30 s) and accurate simulation of basic Knudsen effusion mass spectrometry (KEMS) sampling geometries, allowing for the optimization of orifice sizes and spacings in order to increase transmission and decrease the average number of collisions. This approach was verified with calculation of known transmission factors for simple cylindrical and rectangular orifices. The code has calculated angular distributions of molecules emerging from an orifice and has demonstrated the advantages of a cylindrical orifice to form a directed flow. Finally, the calculations were compared to the analytical analyses of Chatillon et al. for a restricted collimation KEMS system. Future directions were also discussed.

Appendix A—Nomenclature

A, **B**	vectors describing position of segment *u*
a	channel or cylinder width (y-direction)
b	channel or cylinder width (z-direction)
c	distance between two apertures
$\bar{c}$	average number of collisions
D, *Q*, *P*	variables defined by coordinates and direction cosines for convenience
d	channel diameter
DW	distance molecule travels to wall collision
F	fraction of molecules leaving the radiating disk
f	random numbers forming right triangle to generate trigonometric functions of angle δ
G	distance between top of channel and lower aperture
H	distance between lower and upper apertures
h	height of collision point on cylinder
L	channel length
l	channel length
N_θ	flux of molecules vaporizing in angle θ
nc	percent of molecules that escape without collisions
P	probability
p	starting point for vaporizing molecule
$r_{1,2}$	radius of radiating and receiving disk, respectively
r_{ap}	aperture radius
R_i	random number
SW, *SA*, *SB*, *ST*	variables defining trajectory distances
SY, *SZ*	distances from starting point to *y* and *z* coordinates of rectangular channel walls, respectively
u	length of base in right triangle defined by *DW* and *h*
W	transmission factor (i.e., Clausing factor)
y_s,z_s	coordinates of molecule first vaporizing from sample surface
y_{new},z_{new}	point where molecule strikes cylinder wall
y_{old},z_{old}	initial coordinates of molecule's trajectory
α, β, γ	angles that describe molecule's trajectory after wall collision
θ	altitude, angle with x-axis
$\mu_{1,2,3}$	direction cosines for the x-, y-, and z-axes, respectively
ξ	angle of transformation of y- and z-axes after molecule collides with cylinder wall
φ	azimuth angle in y,z-plane
Ψ	angle between vectors **A** and **B**
ω	solid angle

Appendix B—Input and Output Screens

The input and output screens for the Visual Basic for Excel (VBA) code are shown here.

Input Screen

PROGRAM SETTINGS

RUN SIMULATION! Refresh Values

HOW MANY ITERATIONS?	1.0E+06	SHAPE OF PIPE:	
		Round	◉ 1
PLOT TRAJECTORIES?	☑	Rectangular	○
How many?	50	SHAPE OF LOWER ORIFICE:	
		None	○ 2
		Round	◉
		Rectangular	○
SHAPE OF VAPORIZING SOLID:		SHAPE OF UPPER ORIFICE:	
Round	◉ 1	None	○ 2
Rectangular	○	Round	◉
		Rectangular	○

DIMENSIONS

FEATURE	(mm)
A: diameter of vaporizing solid	4.00
B: diameter of pipe	2.00
L: length of pipe	2.00
C: diameter of lower orifice	0.89
D: diameter of upper orifice	3.30
E: distance from solid to pipe	5.00
G: distance to lower orifice	10.00
H: distance to upper orifice	40.00

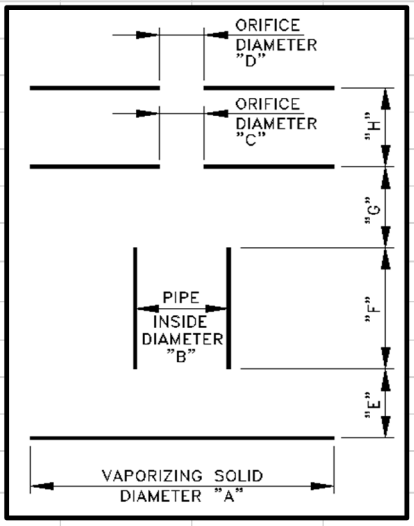

Output Screen

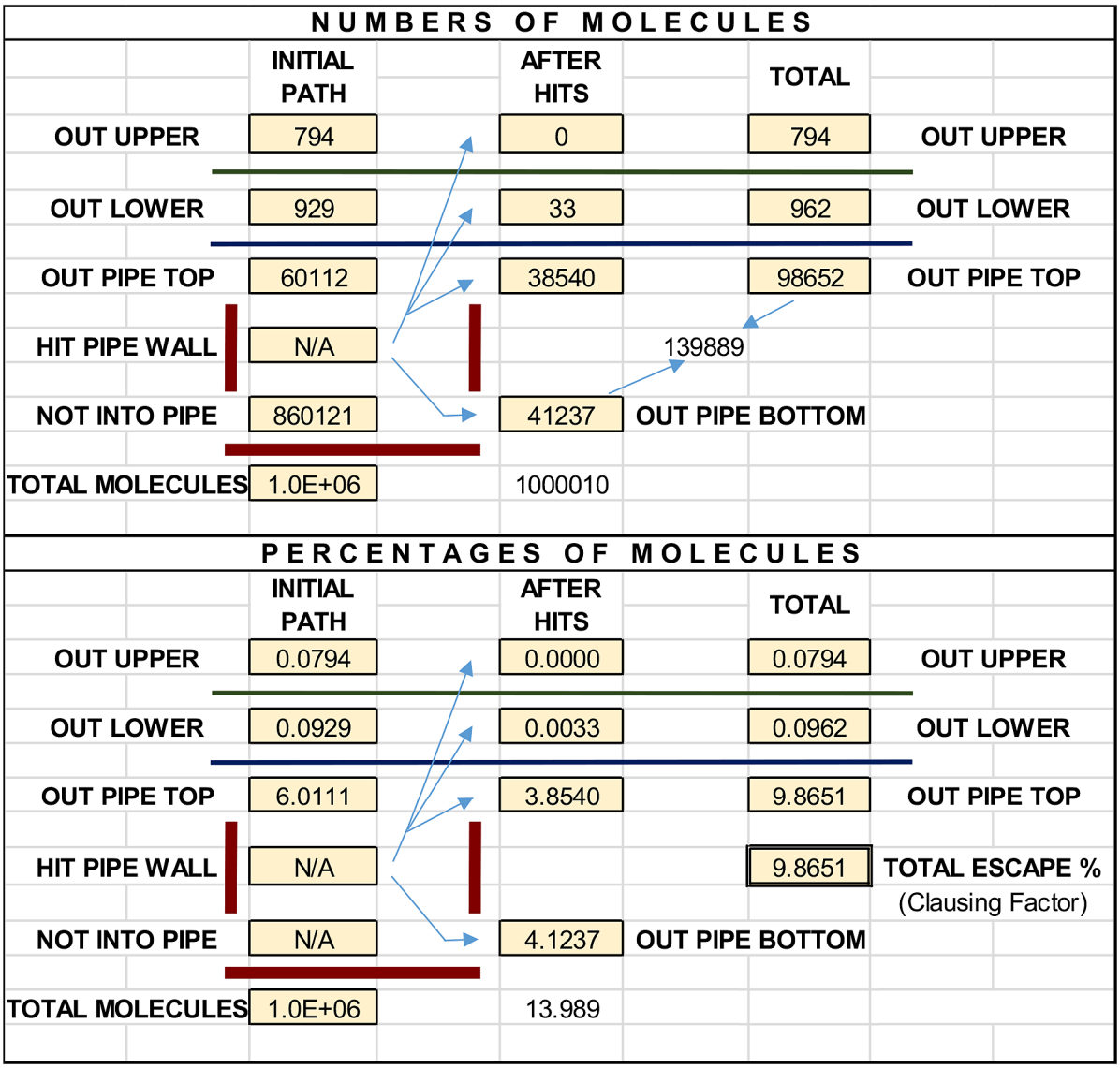

References

1. Drowart, J.; and Goldfinger, P.: Investigation of Inorganic Systems at High Temperature by Mass Spectrometry. Angew. Chem. Int. Ed., vol. 6, no. 7, 1967, pp. 581–596.
2. Copland, E.H.; and Jacobson, N.S.: Measuring Thermodynamic Properties of Metals and Alloys With Knudsen Effusion Mass Spectrometry. NASA/TP—2010-216795, 2010.
3. Chupka, William A.; and Ingrham, Mark G.: Direct Determination of the Heat of Sublimation of Carbon With the Mass Spectrometer. J. Phys. Chem., vol. 59, no. 2, 1955, pp. 100–104.
4. Morland, P.; Chatillon, C.; and Rocabois, P.: High-Temperature Mass Spectrometry Using the Knudsen Effusion Cell. I.—Optimization of Sampling Constraints on the Molecular Beam. High Temp. Mat. Sci., vol. 37, no. 3, 1997, pp. 167–187.
5. Chatillon, Christian, et al.: High-Temperature Mass Spectrometry With the Knudsen Cell: II. Technical Constraints in the Multiple-Cell Method for Activity Determinations. High Temp-High Press, vol. 34, 2002, pp. 213–233.
6. Nuta, Ioana; and Chatillon, Christian: Knudsen Cell Mass Spectrometry Using Restricted Molecular Beam Collimation. I. Optimization of the Beam From the Vaporizing Surface. Rapid Commun. Mass Spectrom., vol. 29, no. 1, 2015, pp. 10–18.
7. Walsh, John W.T.: Radiation From a Perfectly Diffusing Circular Disc (Part I). Proc. Phys. Soc. London, vol. 32, 1920, pp. 59–71.
8. Walsh, John W.T.: Photometry. Constable & Co., London, 1958, pp. 136–144.
9. DeMarcus, W.C.: The Problem of Knudsen Flow. Part 2. Solution of Integral Equation With Probability Kernels. Union Carbide and Carbon Corp., Oak Ridge, TN, 1956.
10. Grimley, Robert T.; Wagner, L.C.; and Castle, Peter M.: Angular Distributions of Molecular Species Effusing From Near-Ideal Orifices. J. Phys. Chem., vol. 79, no. 4, 1975, pp. 302–308.
11. Davis, D.H.: Monte Carlo Calculation of Molecular Flow Rates Through a Cylindrical Elbow and Pipes of Other Shapes. J. Appl. Phys., vol. 31, 1960, pp. 1169–1176.
12. Ward, J.W.; Mulford, R.N.R.; and Bivins, R.L.: Study of Some of the Parameters Affecting Knudsen Effusion. II. A Monte Carlo Computer Analysis of Parameters Deduced From Experiment. J. Chem. Phys., vol. 47, 1967, pp. 1718–1723.
13. Ward, John W.; and Fraser, Malcolm V.: Some of the Parameters Affecting Knudsen Effusion. IV. Monte Carlo Calculations of Effusion Probabilities and Flux Gradients for Knudsen Cells. J. Chem. Phys., vol. 49, 1968, pp. 3743–3750.
14. Ward, John W.; and Fraser, Malcolm V.: Study of Some of the Parameters Affecting Knudsen Effusion. VI. Monte Carlo Analyses of Channel Orifices. J. Chem. Phys., vol. 50, 1969, pp. 1877–1882.
15. Ward, John W.; Bivins, Robert L.; and Fraser, Malcolm V.: Monte Carlo Simulation of Specular and Surface Diffusional Perturbations to Flow From Knudsen Cells. J. Vac. Sci. Technol., vol. 7, 1970, pp. 206–210.
16. Ward, John W.; Fraser, Malcolm V.; and Bivins, Robert L.: Monte Carlo Analysis of the Behavior of Divergent Conical Effusion Orifices. J. Vac. Sci. Technol., vol. 9, 1972, pp. 1056–1061.
17. Jacobson, N.S.: Diffusion of Gases in Capillaries. Ph.D. Thesis, Lawrence Berkeley Lab, 1981.
18. von Neumann, John: Various Techniques Used in Connection With Random Digits. National Bureau of Standards Mathematics Series, vol. 12, 1951, pp. 36–38.
19. Clausing, P.: The Flow of Highly Rarefied Gases Through Tubes of Arbitrary Length. J. Vac. Sci. Technol., vol. 8, 1971, pp. 636–646.
20. Santeler, D.J.; and Boeckmann, M.D.: Combining Transmission Probabilities of Different Diameter Tubes. J. Vac. Sci. Technol. A, vol. 5, 1987, pp. 2493–2496.